Supporting Information

Thermodynamic and kinetic analyses of ion intercalation/deintercalation using different temperatures on NiHCF electrodes for battery electrode deionization

Le Shi [a], Xiangyu Bi [a], Evan Newcomer [a], Derek M. Hall [b], Christopher A. Gorski [a], Bruce E. Logan [a,*]

a. Department of Civil and Environmental Engineering, The Pennsylvania State University, University Park, PA 16802, USA
b. Department of Energy and Mineral Engineering, The Pennsylvania State University, University Park, PA 16802, USA

*Corresponding author. Email: blogan@psu.edu; Tel.: +1-814-863-7908

Number of pages: 7

Number of figures: 4

Number of tables: 2

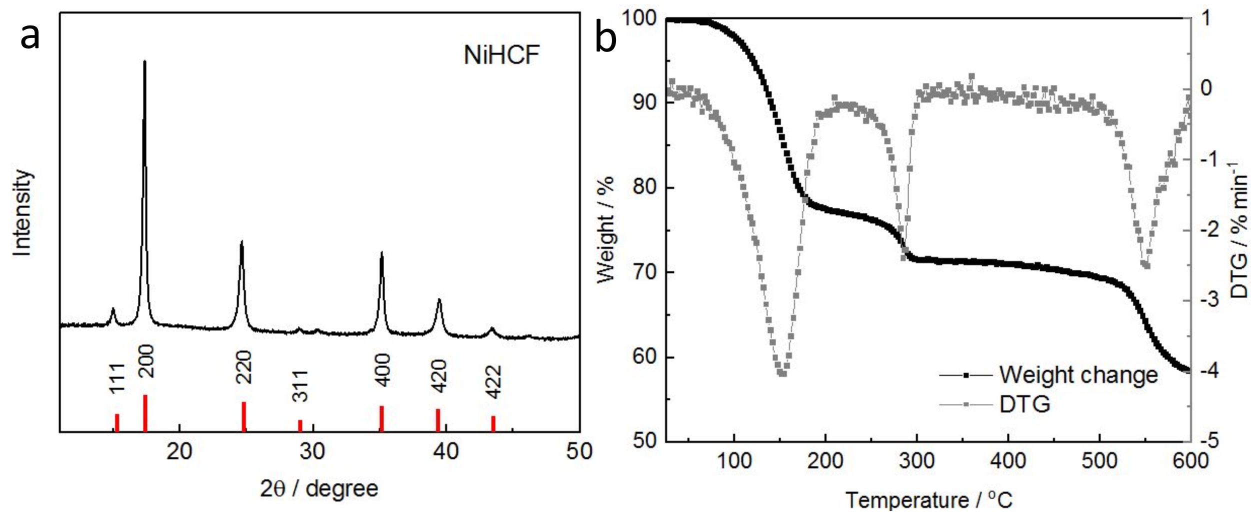

Figure S1. (a) Powder X-ray diffraction (XRD) spectra, and (b) thermogravimetric analysis (TGA) of NiHCF powders.

Table S1. The redox potential (E_{half}, V), the potential difference between the oxidation and reduction reactions (ΔE, V) of NiHCF electrode with each ion at different temperatures (T, °C) recorded in CV (**Figure 1**). The CV data were measured at 2 mV/s.

Ion	T (°C)	E_{red}/V	E_{oxi}/V	E_{half}/V	ΔE/V
Na^+	15	0.358	0.409	0.384	0.051
	35	0.354	0.391	0.373	0.037
	55	0.35	0.379	0.365	0.029
	75	0.341	0.366	0.354	0.025
K^+	15	0.477	0.523	0.499	0.046
	35	0.461	0.504	0.484	0.040
	55	0.455	0.488	0.471	0.033
	75	0.448	0.478	0.463	0.029
Li^+	15	0.125	0.187	0.156	0.062
	35	0.156	0.266	0.211	0.110
	55	0.192	0.261	0.227	0.069
	75	0.198	0.247	0.223	0.049
NH_4^+	15	0.474	0.544	0.509	0.070
	35	0.469	0.515	0.492	0.046
	55	0.473	0.508	0.491	0.035
	75	0.474	0.502	0.488	0.028

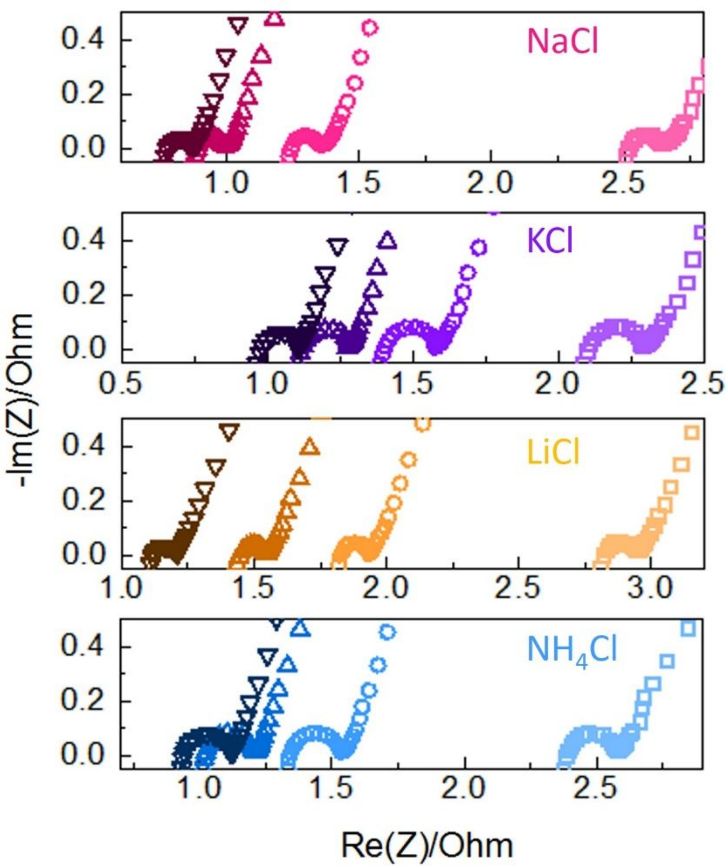

Figure S2. The enlarged figure in the high frequency region of Nyquist plots in **Figure 2.**

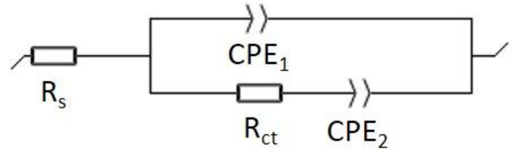

Figure S3. Equivalent circuit corresponding to the generalized Randles model. Rs, the electrolyte resistance; R_{ct}, the charge transfer resistance; CPE_1, constant-phase element corresponding to a capacity at an inhomogeneous electrode surface; CPE_2, constant-phase element corresponding to a diffusion of the cations in an inhomogeneous electrode.

.

$$Z_{CPE}(f) = \frac{1}{Q(j\omega)^{\alpha}}$$

where Q is the CPE with the unit of F $s^{\alpha-1}$, ω is the angular frequency, $\alpha \in [0,1]$ and j is the imaginary number $j^2=-1$. In the particular case where α = 0.5, the impedance is analogous to that of the Warburg element W:

$$Z_W(f) = \frac{\sqrt{2}\sigma}{(j\omega)^{0.5}}$$

where σ is the Warburg coefficient in Ω $s^{-1/2}$.

Table S2. The solution resistance (R_s, Ω), charge transfer resistance (R_{ct}, Ω), the Warburg coefficient (σ, $\Omega/\sqrt{s}$), apparent ion diffusion coefficient (D, cm^2/s), and exchange-current density (i_0) of each sample at different temperatures (T, °C) obtained from Nyquist plots.

Ion	T (°C)	R_s (Ω)	R_{ct} (Ω)	$\sigma(\Omega/\sqrt{s})$	D (cm^2/s)	i_0 (A)
Na^+	15	2.519	0.132	1.438	3.27×10^{-10}	0.188
	35	1.241	0.117	0.859	1.04×10^{-9}	0.227
	55	0.886	0.105	0.664	1.98×10^{-9}	0.269
	75	0.775	0.09	0.651	2.33×10^{-9}	0.333
K^+	15	2.098	0.192	1.131	5.27×10^{-10}	0.129

	35	1.396	0.182	0.737	1.42×10^{-9}	0.146
	55	1.114	0.16	0.572	2.68×10^{-9}	0.177
	75	0.974	0.131	0.545	3.32×10^{-9}	0.229
Li^+	15	2.822	0.118	3.293	0.62×10^{-10}	0.210
	35	1.825	0.104	2.412	1.32×10^{-10}	0.255
	55	1.445	0.097	1.671	3.14×10^{-10}	0.291
	75	1.117	0.088	0.869	1.31×10^{-9}	0.341
NH_4^+	15	2.386	0.196	1.061	5.99×10^{-10}	0.127
	35	1.337	0.196	0.910	9.32×10^{-10}	0.135
	55	1.017	0.188	0.869	1.16×10^{-9}	0.150
	75	0.936	0.182	0.940	1.14×10^{-9}	0.165

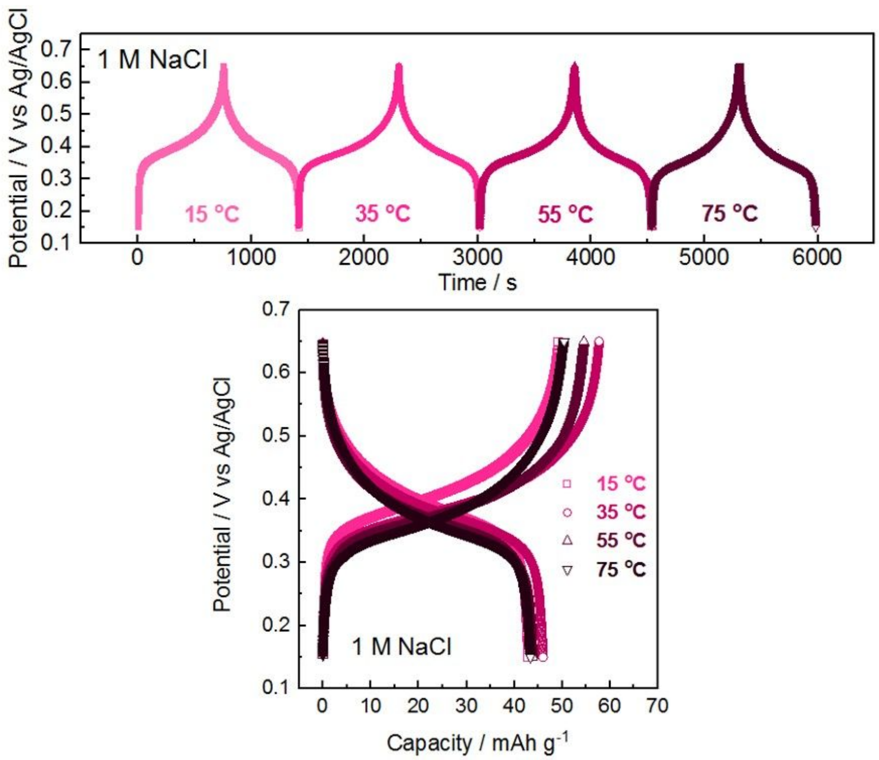

Figure S4. Galvanostatic charge and discharge profiles of NiHCF electrode under varies temperatures with electrolytes of 1M NaCl at 7 mA/30 mg: (a) potential vs time and (b) potential vs capacity profiles.